ORIGINAL ARTICLE

Quantitative assessment of cerebrospinal fluid flow and volume in enlargement of the subarachnoid spaces of infancy using MRI

Chang Y. Ho[1] · Meghana Sankar[2] · Scott Persohn[3] · Stephen F. Kralik[4] · Brian Graner[1] · Paul R. Territo[1,2,3]

Abstract

Background The etiology of enlarged subarachnoid spaces of infancy is unknown; however, there is radiologic similarity with normal pressure hydrocephalus. Adults with normal pressure hydrocephalus have been shown to have altered cerebrospinal (CSF) flow through the cerebral aqueduct.

Objective To explore potential similarity between enlarged subarachnoid spaces of infancy and normal pressure hydrocephalus, we compared MRI-measured CSF flow through the cerebral aqueduct in infants with enlarged subarachnoid spaces of infancy to infants with normal brain MRIs.

Materials and methods This was an IRB approved retrospective study. Clinical brain MRI examinations including axial T2 imaging and phase contrast through the aqueduct were reviewed for infants with enlarged subarachnoid spaces of infancy and for infants with a qualitatively normal brain MRI. The brain and CSF volumes were segmented using a semi-automatic technique (Analyze 12.0) and CSF flow parameters were measured (cvi42, 5.14). All data was assessed for significant differences while controlling for age and sex using analysis of covariance (ANCOVA).

Results Twenty-two patients with enlarged subarachnoid spaces (mean age 9.0 months, 19 males) and 15 patients with normal brain MRI (mean age 18.9 months, 8 females) were included. Volumes of the subarachnoid space ($P < 0.001$), lateral ($P < 0.001$), and third ventricles ($P < 0.001$) were significantly larger in infants with enlarged subarachnoid spaces of infancy. Aqueductal stroke volume significantly increased with age ($P = 0.005$), regardless of group.

Conclusion CSF volumes were significantly larger in infants with enlarged subarachnoid spaces of infancy versus infants with a normal MRI; however, there was no significant difference in CSF flow parameters between the two groups.

Keywords Cerebral aqueduct · Enlargement of subarachnoid space of infancy · Quantitative cerebrospinal fluid flow · 3D volumetry

Introduction

Macrocephaly is a common indication for head imaging in infants. Possible etiologies include hydrocephalus, large subdural hematomas, and enlarged subarachnoid spaces of infancy, which has an incidence of 0.4–0.8 per 1000 live births with a male predominance [1–3]. Enlarged subarachnoid spaces of infancy present as a rapid increase in head circumference around the age of 6 months which stabilizes by approximately 18 months [3, 4]. Affected infants can have transient gross motor and speech delays, with most children becoming neurologically normal [2, 3, 5]. Given minimal long-term consequences and stabilization of increasing head circumference, the term "benign" is typically utilized, such as "benign enlarged subarachnoid spaces of infancy" and "benign external hydrocephalus" in the neurosurgical literature [1–3, 6].

Neuroimaging of enlarged subarachnoid spaces of infancy will typically show enlarged subarachnoid spaces confirmed by traversing cortical veins, as a subdural collection will displace these veins [6, 7]. The enlarged subarachnoid spaces are typically symmetric along the frontal convexities with frontal

✉ Chang Y. Ho
  cyho@iu.edu

1 Department of Radiology and Imaging Sciences, Indiana University School of Medicine, Indianapolis, IN, USA

2 Department of Medicine, Indiana University School of Medicine, Indianapolis, IN, USA

3 Stark Neuroscience Research Institute, Indiana University School of Medicine, Indianapolis, IN, USA

4 Texas Children's Hospital, Houston, TX, USA

interhemispheric fissure enlargement. The lateral and third ventricles are either normal or mildly enlarged [3, 8]. No recognized standard measurement exists to define enlarged subarachnoid spaces of infancy. Lam et al. measured the normal subarachnoid space in infants, with 95% of their population measuring 5 mm or less from the cortex to the superior sagittal sinus [4]. The etiology of enlarged subarachnoid spaces of infancy is currently unknown; however, a prevailing theory is delayed maturity of arachnoid villi, with decreased reabsorption rates leading to accumulation of cerebral spinal fluid (CSF) in the subarachnoid space. Patency of the cranial sutures in neonates allows the head to subsequently enlarge [9].

Bradley et al. suggest that infants with enlarged subarachnoid spaces of infancy eventually become older adults with normal pressure hydrocephalus [10]. Similar to infants with enlarged subarachnoid spaces of infancy, adults with normal pressure hydrocephalus have radiologic findings of enlarged subarachnoid spaces and ventricles as well as enlarged head circumference. Adults with normal pressure hydrocephalus have shown increased CSF stroke volume through the cerebral aqueduct compared to controls [3, 11, 12]. To explore potential similarity between enlarged subarachnoid spaces of infancy and normal pressure hydrocephalus, we utilized MRI to evaluate CSF flow through the cerebral aqueduct in infants with enlarged subarachnoid spaces of infancy compared to infants with normal brain MRIs. Brain parenchymal volume, ventricular volume, and subarachnoid space volumes were also assessed.

Materials and methods

Patient selection

This retrospective study was approved by the institutional review board and complied with the Health Insurance Portability and Accountability Act. While CSF imaging with phase contrast is not routinely performed as part of all brain MRI examinations at our institution, it is added as needed, including in cases of macrocephaly. During the period in which MRI examinations included in this study had been performed (1/2016 to 2/2018), CSF flow imaging had also been performed in a subset of children less than 36 months of age who had otherwise normal MRI examinations. Subject selection was subsequently performed retrospectively with the following criteria: for the enlarged subarachnoid spaces of infancy group, inclusion criteria were (1) MRI referral for macrocephaly, (2) age less than 36 months, (3) measurement of subarachnoid space 5 mm or larger over the frontal convexities, and (4) phase contrast imaging through the cerebral aqueduct. For the normal MRI group, inclusion criteria included (1) MRI brain for multiple indications, where the result was normal by consensus between

2 board certified and fellowship trained neuroradiologists (CH 14 years and SK 10 years of experience, respectively); (2) age less than 36 months; (3) subarachnoid space over the frontal convexities less than 5 mm; and (4) phase contrast imaging through the cerebral aqueduct. Exclusion for both groups included (1) abnormal study for reasons other than enlarged subarachnoid spaces, including large subdural fluid collections, and (2) genetic or syndromic pathology from the electronic medical record.

Imaging technique

All patients except one were imaged according to our institution's protocol with propofol anesthesia provided by the anesthesia department on 1.5 T or 3 T scanners (Siemens Magnetom Avanto and Skyra, Siemens Healthineers, Erlangen, Germany). A single patient in the enlarged subarachnoid spaces of infancy group was papoosed without resulting patient motion on the phase contrast sequence. Scans included axial T2 turbo spin echo (2–4 mm slice thickness, 4500 TR, 112 TE, 120 FA 224×320 matrix), axial EPI diffusion weighted imaging (3 mm slice thickness 7100 TR, 97 TE, 90 FA, 160×160 matrix), and through plane phase contrast imaging performed at the level of the cerebral aqueduct, direction cranial to caudal, Venc = 20 cm/s for one cardiac cycle (24.75 TR, 7.66 TE, 15 FA 256×256 matrix) (Fig. 1).

Image data analysis

The image analyst (MS) who performed region-of-interest measurements was blinded to patient information and patient groupings. All images were de-identified and imported into Analyze 12.0 (AnalyzeDirect, Stilwell, Kansas) for image processing. Each subject had sets of 2 or 3 axial DWI and diffusion 3-scan trace images. All EPI and T2 volumes were loaded separately using the DicomTool into Analyze 12.0.

The 3D voxel registration tool (Analyze 12.0) was used to achieve ventricular symmetry in the axial, coronal, and sagittal planes. All volume images for each subject were subsequently registered with the transformation matrices. The T2 image in each set was also automatically registered to the EPI volume 1 (V1) image and manually corrected. The transformed images were intensity normalized over the interval (0.0–1.0) by dividing each image volume by the maximum value of the image set. A difference image was calculated for each subject by subtracting the maximum volume image by the minimum volume image.

The volume, transformed T2, and difference images were analyzed by a multispectral classification tool which used a feed-forward neural network to segment the background, whole brain, and CSF regions per our previous work [13]. A sample region for each of the three classifications was manually demarcated by the observer, and misclassifications

Fig. 1 Nine-month-old male with macrocephaly. **a** Sagittal T1 weighted image with cut line indicating scan plane of phase contrast imaging through the cerebral aqueduct (*arrow*). **b** Oblique axial phase contrast with flow signal demonstrated in the cerebral aqueduct (*arrow*).
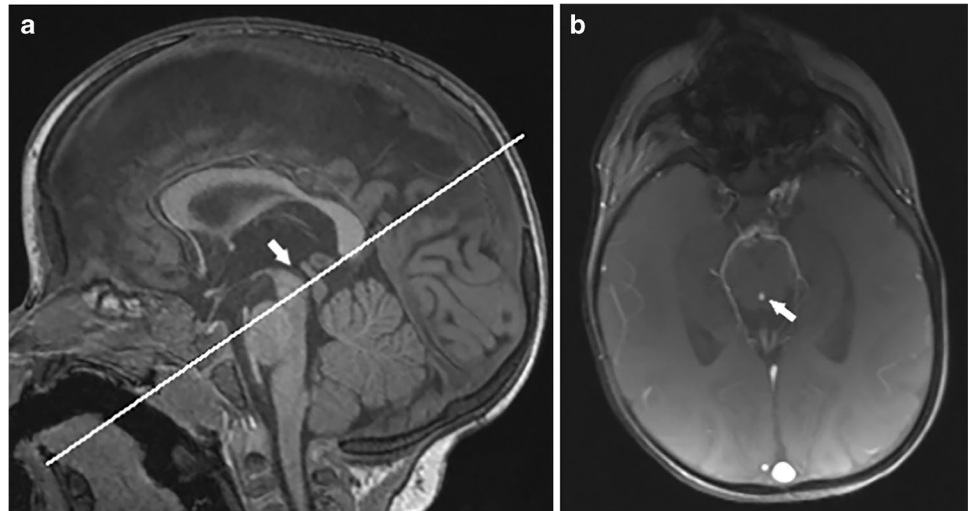
corrected as needed. Only the CSF region required two sample regions, one from a ventricle and another near the edge of the brain. The classifications for the sample slice were reviewed and then propagated for all image slices. In all cases, image segmentation was verified by a board certified neuroradiologist (CH, 14 years experience) and stored for later analysis (Figs. 2 and 3).

The transformed T2 images, background, whole brain, and CSF regions classified by the neural network were further segmented using the volume edit tool (Analyze 12.0). Misclassifications in the eyes and nasal cavities were manually reclassified and excluded from the brain regions. The entire CSF region was extracted using a thresholding technique, where the maximum and minimum range were set based on the intensity values from the captured CSF region. The ventricle spaces in the CSF regions were segmented into lateral, third, and fourth

ventricle regions using a manual drawing and spline editing technique. Finally, volumes for whole brain, subarachnoid space, lateral, third, and fourth ventricle regions were extracted using the region of interest tool (Analyze 12.0). Subjects were classified into enlarged subarachnoid spaces of infancy and normal MRI groups for data analysis.

The total ventricular volume, pixel count, and area were calculated as a sum of the lateral, third, and fourth ventricle region values. Pixel values for the brain regions were calculated according to the following formula (1):

$$V_b(i) = V_T(i) - [V_{CSF}(i) + V_{lateral}(i) + V_{third}(i) + V_{fourth}(i)]$$

where, V_b is the brain region volume, i is the subject, V_T is the total volume, V_{CSF} is the subarachnoid space volume, $V_{lateral}$ is the lateral ventricle region, V_{third} is the third ventricle region, and V_{fourth} is the fourth ventricle region.
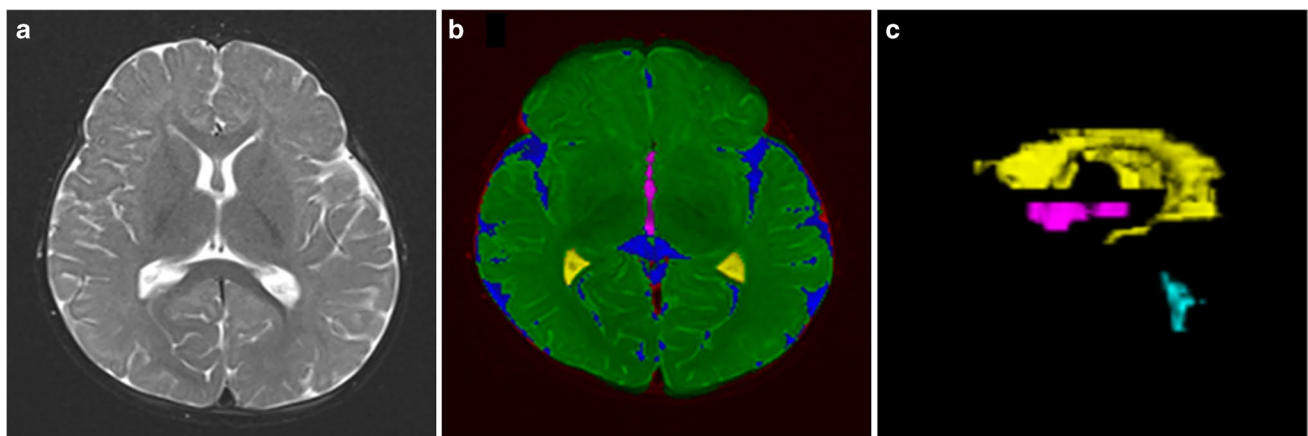

Fig. 2 Sample normal MRI group segmentation images. Eight-month-old female presenting with anisocoria. **a** Axial T2 images. **b** Axial T2 registered EPI images with segmented object regions. **c** 3D ventricular volume images. Object map colors are green, blue, yellow, magenta, and light blue for brain (722.27 ml), subarachnoid space (65.44 ml), lateral ventricle (10.75 ml), third ventricle (0.64 ml), and fourth ventricle (0.86 ml), respectively.
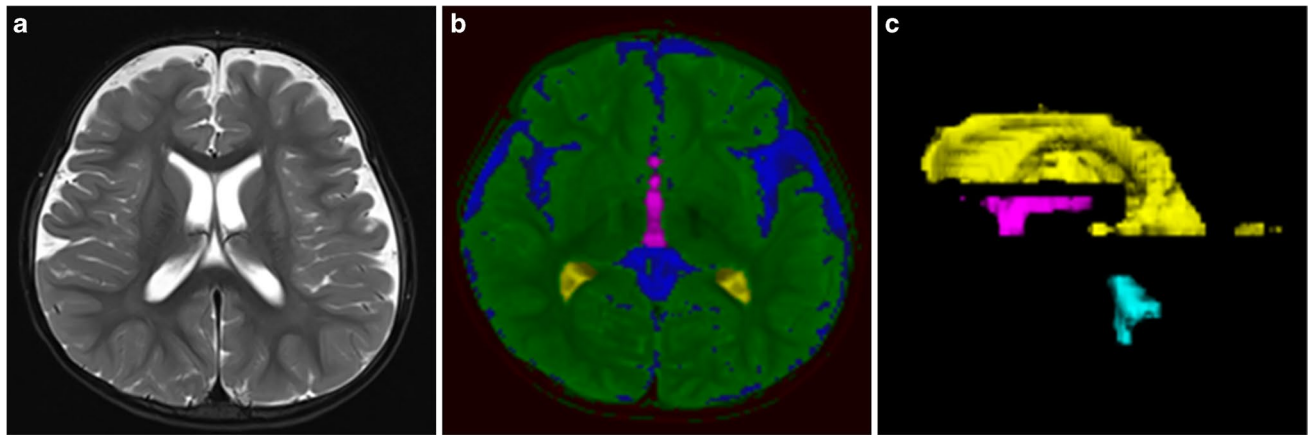
Fig. 3 Sample enlarged subarachnoid spaces of infancy group segmentation images. Twenty-month-old male presenting with macrocephaly and speech delay. **a** Axial T2 images. **b** Axial T2 registered EPI images with segmented object regions. **c** 3D ventricular volume images. Object map colors are green, blue, yellow, magenta, and light blue for brain (1184.99 ml), subarachnoid space (204.46 ml), lateral ventricle (26.45 ml), third ventricle (2.62 ml), and fourth ventricle (1.23 ml), respectively.

Fractional volumes, voxel count, and area were calculated for the subarachnoid and ventricle regions according to the following formula (2):

$$V_f(i,j) = \frac{V(i,j)}{V_b(i) + V_{CSF}(i) + V_{lateral}(i) + V_{third}(i) + V_{fourth}(i)}$$

where, V_f is the fractional volume, i is the subject, j is the region, V is the volume, V_b is the brain region volume, V_{CSF} is the subarachnoid region volume, $V_{lateral}$ is the lateral ventricle region, V_{third} is the third ventricle region, and V_{fourth} is the fourth ventricle region. Fractional volumes were transformed using a log base 10 transformation to accommodate for skewness in fractional data [1,2]. Z-scores were calculated according to the following formula (3):

$$Z(i,j) = \frac{V(i,j) - V_{m,c}(j)}{V_{SD,c}(j)}$$

where, Z is the z-score, V is the volume, i is the subject, j is the region, $V_{m,c}$ is the mean volume of the normal MRI group, and $V_{SD,c}$ is the mean standard deviation of the normal MRI group. The mean, standard deviation, standard error, and average Z-scores were calculated for each segmented region and all fractional volumes and compared between normal MRI and enlarged subarachnoid spaces of infancy subjects. All calculations were performed in Microsoft Excel.

Flow data image analysis

The image analyst (MS) who performed region-of-interest measurements also performed the flow region-of-interest measurements. All images were de-identified and imported into a commercially available cardiovascular imaging software (cvi42, 5.14 Circle Cardiovascular Imaging, Calgary, Canada). The phase contrast images were used for segmentation. The background pons region and the flow contour were manually segmented and propagated for the entire image set. From these analyses, a flow report was generated yielding the parameters for each subject (Table 1). Aqueductal stroke volume (ml) was calculated as the mean of the magnitudes of total forward volume and total backward volume. Subjects were classified into normal MRI and enlarged subarachnoid spaces of infancy groups for data analysis.

Z-scores were calculated similarly to the volume data (4):

$$Z(i,j) = \frac{V(i,j) - V_{m,c}(j)}{V_{SD,c}(j)}$$

where in this formula, V is the value, i is the subject, j is the data value, $V_{m,c}$ is the mean value of the normal MRI group, and $V_{SD,c}$ is the mean standard deviation of the normal MRI group. The mean, standard deviation, standard error, and average z-scores were calculated for each data value for the normal MRI and enlarged subarachnoid spaces of infancy groups.

Statistical analysis

Data were analyzed using SPSS, Version 26 (IBM, Armonk, NY). To control for differences, age and sex were used as covariates in a general linear model univariate test for all measurable variables between groups (ANCOVA). To check for model assumptions and homogeneity between variances, Levene's test and heteroskedasticity F test were utilized. The mean, standard deviation, and standard error of the mean were reported and plotted. Significance was designated at the $P < 0.05$ level.

Table 1 CSF flow parameters through the cerebral aqueduct

Parameter	Unit	Definition
Total forward volume	ml	Positive + negative velocities = positive value (above x-axis)
Total backward volume	ml	Positive + negative velocities = negative value (below x-axis)
Total volume	ml	Total forward volume + total backward volume
Net positive volume	ml	Only positive velocities (above x-axis)
Net negative volume	ml	Only negative velocities (below x-axis)
Regurgitation fraction	%	Ratio between total backward and total forward volume
Volume/min	ml/min	Total volume per minute
Volume/min effective	ml/min	Positive volume per minute
Maximum pressure gradient	mmHg	
Mean pressure gradient	mmHg	
Maximum velocity	cm/s	
Minimum velocity	cm/s	
Maximum mean velocity	cm/s	Value of the phase with the highest mean velocity
Maximum flow	ml/s	
Minimum flow	ml/s	
Aqueductal stroke volume	ml	Mean of absolute values of total forward volume and total backward volume

Results

Between 2016 and 2018, 50 patients were imaged with phase contrast technique with 13 excluded due to abnormal MRI or suspicion for syndromic or genetic pathology. A total of 37 patients were included in the analysis who met the inclusion/exclusion criteria. The sample included 22 patients in the enlarged subarachnoid spaces of infancy group (mean age 9.0 month, range 3–22, 19 males and 3 females) and 15 patients in the normal MRI group (mean age 18.9 months, range 5–36, 7 males and 8 females). Groups were significantly different in age ($P = 0.005$). Clinical indications for MRI in the normal MRI group included febrile seizures ($n = 5$), speech delay ($n = 3$), migraines ($n = 2$), rule out non-accidental trauma ($n = 1$), anisocoria ($n = 1$), alternating exotropia ($n = 1$), torticollis ($n = 1$), and facial venous malformation ($n = 1$); none of which are known to be directly associated with macrocephaly.

Follow-up history in the electronic medical record ranged from none to 6 years after scan for both groups. For the enlarged subarachnoid spaces of infancy group, 6 subjects had no follow-up clinical notes after MRI scan, 4 had speech delay, 2 of which subsequently resolved. The remaining 12 subjects were neurologically normal at the time of the MRI scan and at all available follow-up. For the normal MRI group, 2 subjects had no follow-up clinical notes after MRI, 3 subjects had speech delay, which subsequently resolved for 2 and for which there was no follow-up for 1. The remaining 11 subjects were neurologically normal at MRI scan and available follow-up.

Brain, CSF, and ventricle region volumes

Table 2 shows mean volumes (cm^3) of brain, subarachnoid, lateral ventricle, third ventricle, and fourth ventricle regions for the enlarged subarachnoid spaces of infancy and normal MRI groups. Mean subarachnoid space ($P < 0.001$), mean lateral ventricular ($P < 0.001$), and mean third ventricular ($P < 0.001$) volumes were significantly greater in patients with enlarged subarachnoid spaces of infancy compared to

Table 2 Analysis of covariance for mean measured volumes (ml) for the normal MRI and enlarged subarachnoid spaces of infancy groups with age and sex as a covariate. *Statistically significant ($P < 0.05$)

	Normal MRI ($n = 15$)			Enlarged subarachnoid spaces of infancy ($n = 22$)			
	Mean volume (ml)	Std. error	95% CI	Mean volume (ml)	Std. error	95% CI	P- Value
Brain	944.3	30.5	882.2–1006.4	929.6	34.9	858.6–1000.6	0.76
Subarachnoid	78.1	17.7	42.1–114.2	223.2	20.2	182.0–264.4	<0.001*
Lateral ventricle	12.9	2.7	7.3–18.5	30.3	3.1	23.9–36.7	<0.001*
3rd ventricle	0.6	0.2	0.3–0.9	1.7	0.2	1.3–2.0	<0.001*
4th ventricle	1.0	0.1	0.8–1.2	1.3	0.1	1.1–1.5	0.051

patients with normal MRIs. There were no significant differences in mean brain ($P = 0.13$) or mean fourth ventricular volumes ($P = 0.96$).

For all patients, males ($n = 26$) had significantly greater ($P < 0.001$) brain volumes than females ($n = 11$). There was no significant difference in subarachnoid or ventricular volumes between males and females (Table 3).

For every 1 month increase in age, mean brain volume ($F = 35.363$, $P < 0.001$) was found to increase significantly by 13.292 ml and mean fourth ventricle volume ($F = 30.484$, $P < 0.001$) was found to increase significantly by 0.036 ml. No significant correlations between age and mean volume were found for subarachnoid, lateral ventricle, and third ventricle regions.

CSF flow analysis of the cerebral aqueduct

No significant differences in flow measurements were found between infants with enlarged subarachnoid spaces of infancy and infants with normal MRIs. Similarly, no significant differences between males and females or between infants with enlarged subarachnoid spaces of infancy and infants with normal MRI as a function of sex were found for all parameters.

For every 1 month increase in age, mean total forward volume ($F = 9.585$, $P < 0.005$) increased by 1.31E-03 ml, mean total backward volume ($F = 6.091$, $P < 0.034$) decreased by 7.05E-04 ml, mean total volume ($F = 4.840$, $P < 0.048$) increased by 6.08E-04 ml, and mean stroke volume ($F = 9.118$, $P = 0.005$) increased by 1.01E-03 ml (Table 4). No significant differences between infants with enlarged subarachnoid spaces of infancy and infants with normal MRI by age were found for max pressure gradient, mean pressure gradient, maximum and minimum velocities, and maximum mean velocity.

Discussion

Our study confirms significant increases in subarachnoid space and ventricular size in infants with enlarged subarachnoid spaces of infancy. Although this concept is well

Table 4 Association of age with flow parameters through the cerebral aqueduct for both the enlarged subarachnoid spaces of infancy and normal MRI groups. *Statistically significant ($P < 0.05$)

Parameter	F Statistic	Beta coefficient (ml)	P-Value
Total forward volume	9.59	0.001	*0.004
Total backward volume	6.09	− 0.00071	*0.02
Total volume	4.84	0.00061	*0.04
Net positive volume	9.47	0.001	*0.004
Net negative volume	6.20	− 0.0007	*0.02
MINVOL	6.82	0.17	*0.02
Maximum flow	4.82	0.005	*0.04
Minimum flow	7.75	− 0.006	*0.009
Stroke volume	9.12	0.001	*0.005

recognized clinically, objective confirmation of a previously subjective observation is valuable. We were able to show as expected that all CSF spaces, including subarachnoid space, and lateral, third, and to a lesser extent fourth ventricular volume are enlarged in the enlarged subarachnoid spaces of infancy group; however, brain volumes were not decreased in enlarged subarachnoid spaces of infancy patients. This is pertinent, as decreases in brain volume do not appear to be a factor in the symptoms of developmental delay that can be seen transiently in infants with enlarged subarachnoid spaces of infancy. This contrasts with severe long-standing hydrocephalus which can result in white matter volume loss and subsequent pervasive developmental delay and cerebral palsy.

We were not able to find significant differences in flow parameters across the cerebral aqueduct in our study between enlarged subarachnoid spaces of infancy and infants with normal MRIs. While we are unable to demonstrate similarity between enlarged subarachnoid spaces of infancy and adult normal pressure hydrocephalus, it should be noted that the cranial sutures are able to accommodate for increases in intracranial volume and pressure in infancy, by increasing head circumference. Cranial suture fusion in adulthood results in a loss of accommodation of increased intracranial pressure [14, 15]. The stretching of cranial sutures and corresponding increase in

Table 3 Analysis of covariance for mean measured volumes (ml) comparing females and males with age as a covariate. *Statistically significant ($P < 0.05$)

	Females ($n = 11$)			Males ($n = 26$)			
	Mean volume (ml)	Std. error	95% CI	Mean volume (ml)	Std. error	95% CI	P-Value
Brain	855.2	36.0	781.8–928.5	1018.8	23.7	970.5–1057.0	0.001*
Subarachnoid	147.6	20.9	105.1–190.2	153.7	13.8	125.7–181.8	0.81
Lateral ventricle	24.6	3.2	18.0–31.2	18.6	2.1	14.3–22.9	0.13
3rd ventricle	1.2	0.2	0.8–1.5	1.1	0.1	0.9–1.4	0.93
4th ventricle	1.1	0.1	0.9–1.3	1.2	0.1	1.0–1.3	0.82

head size may normalize any differences in CSF flow across the cerebral aqueduct in enlarged subarachnoid spaces of infancy patients. With fusion of the cranial sutures in adulthood, this accommodation is lost, which may lead to increased aqueductal stroke volume in NPH subjects versus controls.

As a result of the range of ages in our study, several variables can be correlated with normal aging and sex in the first few years of life. As previously described, brain volumes for male infants were larger than female infants [16]. New knowledge resulting from our study is that stroke volume increases with age in the first years of life without associated increases in velocity, suggesting that the cerebral aqueduct itself increases in size.

Alternatively, recent literature suggests a different theory as to the etiology of enlarged subarachnoid spaces of infancy. Sainz et al. found that 15/17 subjects with enlarged subarachnoid spaces of infancy had dural venous sinus anomalies [17]. In a larger cohort of 97 patients, Cinalli et al. confirmed a significant correlation of both the rate and grade of dural venous sinus stenosis of enlarged subarachnoid spaces of infancy patients compared to a control group [18]. The pathophysiology these authors suggest is that dural venous sinus stenosis raises intravenous and intracranial pressure, leading to enlarged head circumference. Non-invasive methods of functional venous analysis may help elucidate whether this etiology will supplant the previous theory of immature arachnoid villi. This may be a future field of study for the etiology of enlarged subarachnoid spaces of infancy.

The current study had several limitations: (1) while the included comparison patients had no visible abnormality on MRI, it is not possible to prove that these infants had no neurologic abnormality. (2) Our study was not powered to detect subtle differences in volumes or flows. Previous work has shown that phase contrast estimates of net flow rates in cardiac studies are impacted by turbulent flow [19]. Given the small size of the aqueduct and susceptibility to turbulent flow, as well as the small sample sizes used in the current study, additional work may be needed to understand if these parameters yield meaningful measures in enlarged subarachnoid spaces of infancy subjects. (3) We were not able to effectively age match the two cohorts, with the normal MRI group significantly older by nearly 10 months. However, we did control for age statistically, and we did not find spurious low brain volumes in the younger enlarged subarachnoid spaces of infancy group.

Conclusion

Children with enlarged subarachnoid spaces of infancy have larger subarachnoid spaces and ventricles compared to infants with normal MRIs. There was no significant difference in brain volumes between the two groups, suggesting that any associated developmental delays are independent of brain volume. Although there were no significant differences in CSF flow parameters between the two groups, we did find increased aqueductal stroke volume with age.

Data Availability Data for this study is not publicly available to protect subject privacy and conform to HIPAA privacy rules. A limited dataset may be made available from the corresponding author on request.

Declarations

Ethics approval This research study was conducted retrospectively from data obtained for clinical purposes. We consulted with the IRB of Indiana University School of Medicine who determined that our study did not need ethical approval. An IRB official waiver of ethical approval was granted from the IRB of Indiana University.

Informed consent Informed consent was waived by the IRB of Indiana University. No identifying information was included in the manuscript.

Conflict of interest The authors declare no competing interests.

References

1. Wiig US, Zahl SM, Egge A, Helseth E, Wester K (2017) Epidemiology of benign external hydrocephalus in Norway-a population-based study. Pediatr Neurol 73:36–41. https://doi.org/10.1016/j.pediatrneurol.2017.04.018

2. Marino MA, Morabito R, Vinci S et al (2014) Benign external hydrocephalus in infants. A single centre experience and literature review. Neuroradiol J 27:245–250. https://doi.org/10.15274/NRJ-2014-10020

3. Zahl SM, Egge A, Helseth E, Wester K (2011) Benign external hydrocephalus: a review, with emphasis on management. Neurosurg Rev 34:417–432. https://doi.org/10.1007/s10143-011-0327-4

4. Lam WW, Ai VH, Wong V, Leong LL (2001) Ultrasonographic measurement of subarachnoid space in normal infants and children. Pediatr Neurol 25:380–384. https://doi.org/10.1016/s0887-8994(01)00349-6

5. Halevy A, Cohen R, Viner I, Diamond G, Shuper A (2015) Development of infants with idiopathic external hydrocephalus. J Child Neurol 30:1044–1047. https://doi.org/10.1177/0883073814553273

6. Tucker J, Choudhary AK, Piatt J (2016) Macrocephaly in infancy: benign enlargement of the subarachnoid spaces and subdural collections. J Neurosurg Pediatr 18:16–20. https://doi.org/10.3171/2015.12.PEDS15600

7. Caré MM (2021) Macrocephaly and subdural collections. Pediatr Radiol 51:891–897. https://doi.org/10.1007/s00247-020-04848-1

8. Kumar R (2006) External hydrocephalus in small children. Childs Nerv Syst 22:1237–1241. https://doi.org/10.1007/s00381-006-0047-1

9. Orrù E, Calloni SF, Tekes A, Huisman TAGM, Soares BP (2018) The child with macrocephaly: differential diagnosis and neuroimaging findings. AJR Am J Roentgenol 210:848–859. https://doi.org/10.2214/AJR.17.18693

10. Bradley WG (2015) CSF flow in the brain in the context of normal pressure hydrocephalus. AJNR Am J Neuroradiol 36:831–838. https://doi.org/10.3174/ajnr.A4124

11. Lindstrøm EK, Ringstad G, Mardal K-A, Eide PK (2018) Cerebrospinal fluid volumetric net flow rate and direction in idiopathic normal pressure hydrocephalus. Neuroimage Clin 20:731–741. https://doi.org/10.1016/j.nicl.2018.09.006

12. Shanks J, Markenroth Bloch K, Laurell K et al (2019) Aqueductal CSF stroke volume is increased in patients with idiopathic normal pressure hydrocephalus and decreases after shunt surgery. AJNR Am J Neuroradiol 40:453–459. https://doi.org/10.3174/ajnr.A5972

13. Ho CY, Kindler JM, Persohn S et al (2020) Image segmentation of plexiform neurofibromas from a deep neural network using multiple b-value diffusion data. Sci Rep 10:17857. https://doi.org/10.1038/s41598-020-74920-1

14. Wilkinson CC, Stence NV, Serrano CA et al (2020) Fusion patterns of major calvarial sutures on volume-rendered CT reconstructions. J Neurosurg Pediatr 1–10 https://doi.org/10.3171/2019.11.PEDS1953

15. Pong AC, Jugé L, Bilston LE, Cheng S (2017) Development of acute hydrocephalus does not change brain tissue mechanical properties in adult rats, but in juvenile rats. PLoS One 12: e0182808. https://doi.org/10.1371/journal.pone.0182808

16. Knickmeyer RC, Xia K, Lu Z et al (2017) Impact of demographic and obstetric factors on infant brain volumes: a population neuroscience study. Cereb Cortex 27:5616–5625. https://doi.org/10.1093/cercor/bhw331

17. Sainz LV, Zipfel J, Kerscher SR et al (2019) Cerebro-venous hypertension: a frequent cause of so-called "external hydrocephalus" in infants. Childs Nerv Syst 35:251–256. https://doi.org/10.1007/s00381-018-4007-3

18. Cinalli G, di Martino G, Russo C et al (2021) Dural venous sinus anatomy in children with external hydrocephalus: analysis of a series of 97 patients. Childs Nerv Syst 37:3021–3032. https://doi.org/10.1007/s00381-021-05322-5

19. O'Brien KR, Cowan BR, Jain M et al (2008) MRI phase contrast velocity and flow errors in turbulent stenotic jets. J Magn Reson Imaging 28:210–218. https://doi.org/10.1002/jmri.21395